International Conference on Space Optics—ICSO 2018

Chania, Greece

9–12 October 2018

Edited by Zoran Sodnik, Nikos Karafolas, and Bruno Cugny

Antimonides Type-II superlattice digital focal plane arrays for Space remote sensing instruments

Sarath Gunapala

David Ting

Alexander Soibel

Arezou Khoshakhlagh

et al.

International Conference on Space Optics — ICSO 2018, edited by Zoran Sodnik, Nikos Karafolas, Bruno Cugny, Proc. of SPIE Vol. 11180, 111803T · © 2018 ESA and CNES · CCC code: 0277-786X/18/$18 · doi: 10.1117/12.2536056

Antimonides Type-II Superlattice Digital Focal Plane Arrays for Space Remote Sensing Instruments

Sarath Gunapala, David Ting, Alexander Soibel, Arezou Khoshakhlagh,
Sir Rafol, Cory Hill, Anita Fisher, and Brian Pepper

Center for Infrared Photodetectors, Jet Propulsion Laboratory, California Institute of Technology
Pasadena, California, USA

Kwong-Kit Choi

US Army Research, Development and Engineering Command, Army Research Laboratory
Adelphi, Maryland, USA

Arvind D'Souza and Christopher Masterjohn

DRS Network & Imaging Systems, Inc.
Cypress, California, USA

Sachidananda Babu and Parminder Ghuman
NASA Earth Science Technology Office
Greenbelt, Maryland, USA

ABSTRACT

In this paper, we report our recent efforts in achieving high performance in Antimonides type-II superlattice (T2SL) based infrared photodetectors using the barrier infrared detector (BIRD) architecture, resonator pixel light coupling mechanism, and digital read out integrated circuits (DROICs).

Keywords: type-II superlattice, infrared detector, high quantum efficiency, high dynamic range, focal plane array

INTRODUCTION

In this presentation, we will report our recent efforts in achieving high performance in Antimonides type-II superlattice (T2SL) based infrared photodetectors using the barrier infrared detector (BIRD) architecture. The recent emergence of barrier infrared detectors such as the nBn [1] and the XBn [2] have resulted in mid-wave infrared (MWIR) and long-wave infrared (LWIR) detectors with substantially higher operating temperatures than previously available in III-V semiconductor based MWIR and LWIR detectors. The initial nBn devices used either InAs absorber grown on InAs substrate, or lattice-matched InAsSb alloy grown on GaSb substrate, with cutoff wavelengths of ~3.2 μm and ~4 μm, respectively. While these detectors could operate at much higher temperatures than existing MWIR detectors based on InSb, their spectral responses do not cover the full (3 – 5.5 μm) MWIR atmospheric transmission window. There also have been nBn detectors based on the InAs/GaSb T2SL absorber [3,4].

BARRIER INFRARED DETECTORS

Much has been discussed in the literature about the nBn and related devices, including XBn barrier photodetector [2,5,6-8], and unipolar barrier photodiode [9], since the publication of the influential paper entitled "nBn detector, an infrared detector with reduced dark current and higher operating temperature" by Maimon and Wicks in 2006 [1]. Common to this family of devices is the unipolar barrier. The term "unipolar barrier" was used recently to describe a barrier that can block one carrier type (electron or hole) but allows the un-impeded flow of the other [10-12]. The concept of the unipolar barrier has been around long before they are called as such. The double-heterostructure (DH) laser, which makes use of a pair of complementary unipolar barriers, was first described in 1963 [13,14], soon after the birth of the concept of heterostructure devices.

The ideal nBn structure would have two n-type region (n) separated by a larger bandgap, undoped barrier layer (B), where the n-B heterojunctions have a larger conduction band offsets and zero valence band offsets. Such a barrier would block majority carrier electrons, but pass photogenerated holes. The nBn and XBn device structures are reminiscent of that proposed by Anthony White in 1983 [15]. The nBn infrared detector is designed to reduce dark current (noise) without impeding photocurrent (signal). Central to the nBn operation is the strong suppression of generation-recombination (G-R) dark current due to Shockley-Read-Hall (SRH) processes. The nBn infrared detector is designed to reducing dark current (noise) without impeding photocurrent (signal).

Another important aspect of nBn and related structures is their effectiveness in reducing surface leakage current. The top surface of the active narrow gap absorber in the nBn detector is covered by the wide band gap barrier layer, and therefore does not need additional passivation to suppress surface leakage [1]. In a focal plane array (FPA) configuration, the array of top contacts could be defined by etching through the top contact layer but not the barrier layer [1]. In this configuration, the narrow gap absorber is not exposed, and therefore does not contribute to surface leakage. Finally, even in a deep-etched mesa configuration, where the side walls of the narrow gap absorber are fully exposed, the barrier can still block electron surface leakage effectively [1, 9,16-19]. The unipolar barrier based design is not limited to the nBn or XBn. The complementary barrier infrared detector (CBIRD) demonstrated by David Ting *et al*. [12] uses a pair of electron and hole unipolar barriers with LWIR InAs/GaSb superlattice to achieve near diffusion limited performance.

Realization of unipolar barrier infrared detector structures typically involves a set of rather stringent requirements. Designing an nBn IR detector requires a matching pair of absorber and barrier materials with the following properties: (1) their valence band edges must be approximately the same to allow un-impeded hole flow, while their conduction band edges should have a large difference to form an electron barrier, (2) the absorber should have the desired band gap, (3) the absorber should be very closely lattice-matched to the substrate to ensure high material quality and low defect density, and (4) the barrier should also be approximately lattice-matched to the substrate, although the requirement here is less stringent since a barrier thickness of 1,000 to 2,000 Å is typically sufficient, and therefore a modest amount of strain can be tolerated.

The conditions favorable for constructing nBn structures are found in the nearly lattice-matched semiconductors of InAs, GaSb, and AlSb, commonly referred to as the 6.1 Å material system since InAs, GaSb, and AlSb all have lattice constants of approximately 6.1 Å. They are also commonly referred to as the antimonides (InAs is included by virtue of being closely lattice-matched to GaSb and AlSb).

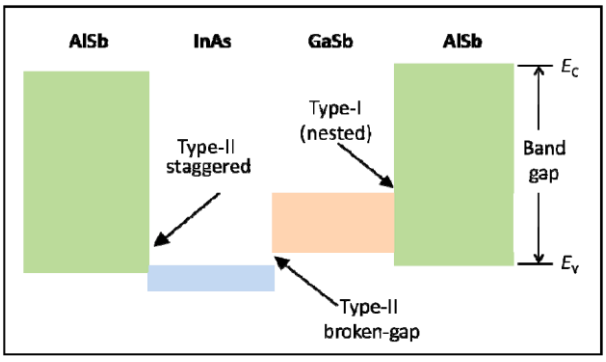

Figure 1. Schematic illustration of the energy band alignment in the nearly lattice matched InAs/GaSb/AlSb material system. The solid colored rectangles indicate the relative positions of the InAs, GaSb and AlSb energy band gaps. Three types of band alignment are available in this material system: (1) type-I (nested) band alignment between GaSb and AlSb, (2) type-II staggered alignment between InAs and AlSb, and (3) type-II broken gap (or type-III) alignment between InAs and GaSb.

As illustrated in Fig. 1, the 6.1 Å materials offers a variety of band offsets, with considerable flexibility in forming a rich variety of alloys and superlattices. Together with their alloys with InSb, GaAs, and AlAs, the 6.1 Å semiconductors provided a great degree of versatility for constructing heterostructure devices. In particular, we note that AlSb exhibits large condition band offsets, but has relatively smaller valence band offsets, to InAs and GaSb, thus providing a good starting point for building nBn detector structures. The 6.1 Å or antimonide materials can be grown on InAs or GaSb

substrates, GaSb is available in 2", 3", 4" and 6" diameters formats. Most of the nBn and related device structures published in the literature to date have been implemented in the antimonide material system. BIRDs have been implemented for bulk InAs [19], InSb, InAsSb, InGaAsSb, InAsPSb, and HgCdTe, as well as for InAs/GaSb type-II superlattice (T2SL) and for the InAs/InAsSb T2SL [20]. An important aspect of the nBn detector (and unipolar barrier detector architecture in general) is the ability to block majority carriers without impeding the flow of minority carriers.

RESONATOR PIXEL

In the past, achieving a high quantum efficiency (QE) in infrared detection requires a thick absorber and a large absorption coefficient α. This requirement severely limits the choice of materials when the detection wavelength is longer than 8 μm. If high QE can be obtained even with a thin absorber layer and a small α, it will open up many more possibilities. Materials that were once regarded as problematic, such as those with small α, short minority carrier diffusion length, or small critical growth thickness, can now be considered. To realize this possibility, we propose a resonator pixel T2SL barrier infrared detector structure that can trap and store incident light until it is absorbed. With a perfect trap, the QE will no longer be limited by the material thickness or α. To make an effective trap, the light must not transmit out of the detector when it hits the detector boundaries, and it must not interfere destructively with the incident light or other light already present in the detector. We call this design the "resonator pixel". An EM model developed to simulate resonator pixels can accurately predict the photo-response of actual fabricated infrared detectors. [21-23].

To understand the proposed detector structure, let's consider a detector slab in Fig. 2(a) with a metal reflector on top, and light is incident from the bottom substrate. With this standard detector geometry, light will bounce up and down between the metal and the substrate/air interface, with which a Fabry-Perot etalon (FPE) is formed. However, this FPE does not confine photons effectively because the substrate transmission can be large, and because optical interference can either aid or suppress the escape of light at the interface, resulting in QE oscillations that are centered about its classical value. If the detector top surface contains instead a set of diffractive elements (DEs) as shown in Fig. 2(b), light will be diffracted at an angle. And if this angle is larger than the critical angle at the substrate/air interface (~16° for GaSb), then light will be totally internally reflected at the substrate and will stay inside the detector. When the same is also true for all other detector sidewalls, then light will be totally confined. To account for interference effects, the size and shape of the detector volume must be adjusted such that the scattered optical paths form a constructive interference pattern inside the detector. Under this condition, the newly incident light will be able to reinforce the light already under circulation, and the optical energy can be accumulated and stored in the detector as in a resonator. Therefore, by designing the detector into a resonator with a diffractive surface, an effective photon trap can be obtained.

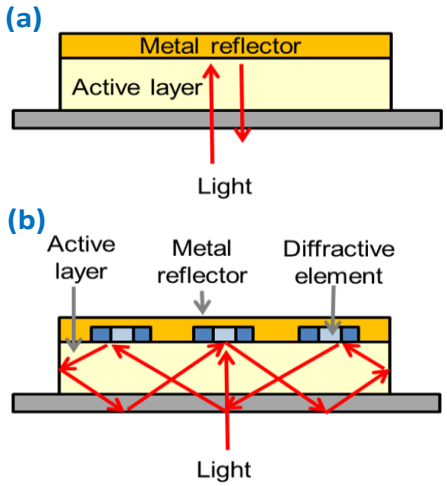

Figure 2. (a) In conventional detectors, incident light travels up and down the material slab, creating Fabry-Perot oscillations. (b) In light-trapping resonator detector structures, light circulates inside each pixel, making the path length longer.

Rigorous 3D electromagnetic (EM) simulation capabilities have been developed to aid the design and modeling of photodetector pixels [21]. The model has been validated through extensive comparisons with experimental results on different types of infrared detectors, including quantum well infrared photodetectors (QWIPs) and T2SL infrared detectors. We now use EM modeling to examine how the resonator pixel concept can be used to enhance the performance of LWIR BIRDs. The simplest and the most well-known unipolar barrier infrared detector architecture is the nBn. The nBn has the advantage of having very well-behaved surface properties, which lead to good dark current characteristics and low 1/f noise (temporal stability). The one drawback is that when used with LWIR T2SL absorbers (necessary for achieving long cutoff wavelengths), which have short hole diffusion lengths, the absorbers need to be kept fairly thin (below the diffusion length), which in turn limits the attainable QE. The light trapping resonator pixel concept offers a very effective solution in this case. For many imaging and spectral imaging applications, light incident at a relatively large angle needs to be considered. For an example, we have calculated the spectral response for 35º incident angle. The calculated 35º-incidence spectral QE has the same shape as the normal-incidence QE. In general, it is safe to say that the resonator-pixel enhancement has fairly weak angular dependence. This is an advantage over layered anti-reflection coating, which tends to show strong angular dependence [22-23].

DIGITAL READ OUT INTEGRATED CIRCUIT

Infrared FPAs generally use non-silicon detector arrays to convert the infrared signal into an electrical signal. These detector arrays are hybridized via indium bump bonding process to a read out integrated circuit (ROIC). Conventional ROICs are based on analog electronic circuits. The modern ROICs are digital ROICs (DROICs). Conventional analog ROICs store charges at individual ROIC pixels and route them out via output taps to off-chip analog-to-digital converters (ADCs) or route them to on-chip column parallel ADCs. This method requires a very large ROIC in-pixel well depth to achieve high signal-to-noise-ratio (SNR). In DROICs the charges get digitized at ROIC individual pixel level with a counter by incrementing each time a small charge bucket gets filled. Ideally, this could provide a very high effective well depth for DROIC pixels compared to conventional analog ROIC pixels. Total well depth of DROIC pixel is given by the size of the charge bucket times the number of counts of the in-pixel counter [24-25].

The ultimate sensitivity (i.e., highest SNR) of an infrared FPA is determined by the maximum well depth of the ROIC pixels assuming the total noise of the FPA is determined by the shot noise (i.e., statistical fluctuations of the signal) of the photocurrent. Therefore, to achieve the maximum SNR,

$$SNR_{Max} = \frac{Signal_{Max}}{Noise} = \sqrt{Well\ Depth_{Max}}$$

Where, $Signal_{Max}$ is the maximum signal and noise is Poisson process limited statistical variation associated with the photocurrent. Thus, a maximum well depth of 25 million electrons yields SNR of 5,000 and well depth of 100 million electrons yields SNR of 10,000. Therefore, a DROIC with higher bit counter could provide a higher SNR or could operate a DFPA at higher operating temperature with same SNR as a conventional FPA (i.e., same detector array with an analog ROIC).

SUMMARY

A T2SL LWIR BIRD FPA could easily operates at 20K higher operating temperature (HOT) (i.e. compared to QWIP FPA) due to the strong suppression of G-R dark current due to SRH processes as explained earlier. The light trapping resonator pixel concept offers a very effective solution to increase the QE of LWIR T2SL BIRDs. We could conservatively expect the resonator pixel to yield QE of >50% and lower dark current, thus, it can achieve comparable SNR (i.e., as conventional LWIR QWIP FPA) while operating at 20K higher temperature. Another 20K higher operating temperature advantage can be achieved when we further improve the performance by hybridizing the T2SL LWIR BIRD detector array to the high-dynamic range DROIC from DRS. Therefore, a T2SL LWIR BIRD DFPA can easily operates at ~60K higher operating temperature compared to a conventional LWIR FPA. We calculated the noise equivalent temperature difference (NEΔT) as a function of the ROIC well depth for the two Landsat spectral bands 10.3-11.3 μm and 11.5-12.5 μm at different resonator pixel BIRD FPA (see Figure 3). Figure 3 clearly shows, the resonator pixel BIRD digital focal plane arrays (i.e., with 0.5-1 billion electrons well depths) can operate easily at 100K with ~20 mK NEDT.

This is a very significant improvement of the FPA operating temperature compared to the previous Landsat thermal imaging instrument.

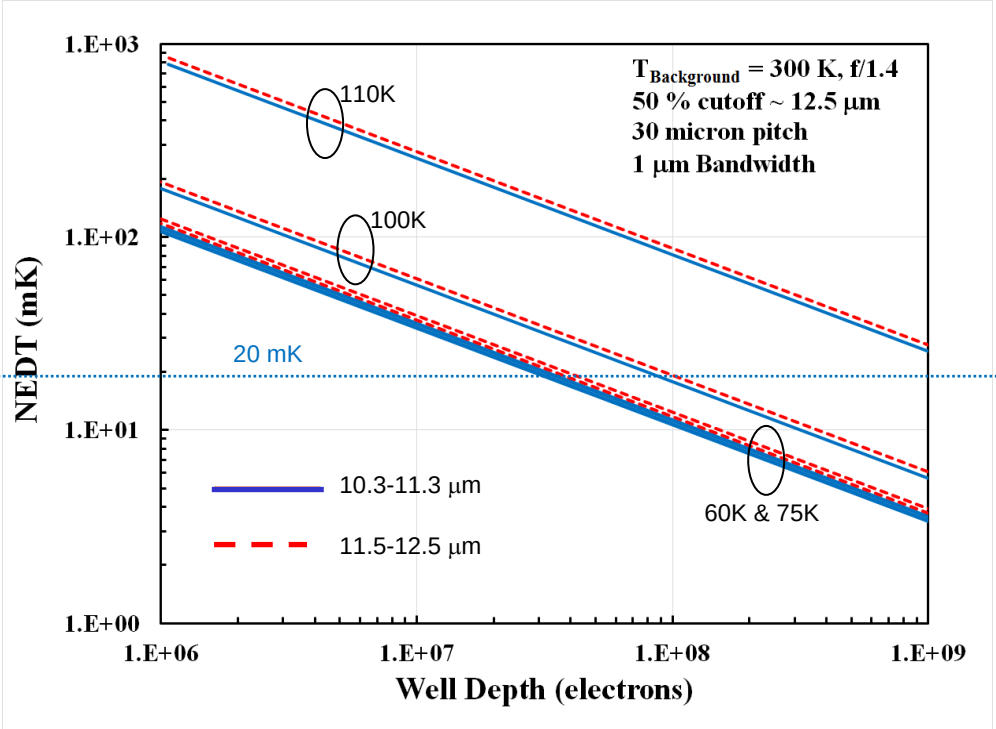

Figure 3. NEΔT as a function of ROIC well depth for resonator pixel BIRD focal plane array operating at 60 – 100 K operating temperatures. Solid blue and dashed red lines represent the two Landsat bands 10.3-11.3 and 11.5-12.5 µm respectively. Blue dotted line represents the 20 mK NEΔT as a guide to the eye.

ACKNOWLEDGEMENT

This work is funded by the NASA Earth Science Technology Office. The research described in this paper was carried out at the Jet Propulsion Laboratory, California Institute of Technology, under a contract with the National Aeronautics and Space Administration.

REFERENCES

[1] S. Maimon and G. W. Wicks, "nBn detector, an infrared detector with reduced dark current and higher operating temperature", Appl. Phys. Lett. 89, 151109 (2006).
[2] P. C. Klipstein, "XBn barrier photodetectors for high sensitivity and high operating temperature infrared sensors," Proc. SPIE 6940, 6940–2U (2008).
[3] Eliezer Weiss, Olga Klin, Steve Grossmann, Noam Snapi, Inna Lukomsky, Daniel Aronov, Michael Yassen, Eyal Berkowicz, Alex Glozman, Philip Klipstein, Avraham Fraenkel, Itay Shtrichman, "InAsSb-based XBnn bariodes grown by molecular beam epitaxy on GaAs", J. Crystal Growth 339(1), 31–35 (2012).
[4] J. F. Klem, S.R. Kurtz, A. Datye, "Growth and properties of GaAsSb/InGaAs superlattices on InP", J. Crystal Growth 111(1-4), 628-632 (1991).
[5] Hiroshi Inada, Kouhei Miura, Hiroki Mori, Youichi Nagai, Yasuhiro Iguchi And Yuichi Kawamura, "Low Dark Current SWIR Photodiode with InGaAs/GaAsSb Type II Quantum Wells Grown on InP Substrate", SEI Technical Review 70, 100-102 (2010).

[6] Baile Chen and Archie L. Holmes, Jr., "InP-based short-wave infrared and midwave infrared photodiodes using a novel type-IIstrain-compensated quantum well absorption region", Optics Letters 38(15) 2750 (2013).
[7] D. L. Smith, T. C. McGill, and J. N. Schulman, "Advantages of the HgTe-CdTe superlattice as an infrared detector material", Appl. Phys. Lett. 43(2), 180-182 (1983).
[8] C. H. Grein, P. M. Young, and H. Ehrenreich, "Minority carrier lifetimes in ideal InGaSb/InAs superlattices", Appl. Phys. Lett. 61(24), 2905 (1992).
[9] L. Bürkle and F. Fuchs, "InAs/(GaIn)Sb superlattices: a promising material system for infrared detection" in Handbook of Infrared Detection Technologies (M. Henini and M. Razeghi, Ed.), pp. 159-189. Elsevier Science, Oxford (2002).
[10] David Z.-Y. Ting, Alexander Soibel, Linda Höglund, Jean Nguyen, Cory J. Hill, Arezou Khoshakhlagh, and Sarath D. Gunapala, "Type-II Superlattice Infrared Detectors" in Semiconductors and Semimetals, Vol. 82, Advances in Infrared Photodetectors (S. Gunapala, D. Rhiger, and C. Jagadish, Ed.), 1-57, Elsevier Academic Press (2011).
[11] E. H. Steenbergen, B. C. Connelly, G. D. Metcalfe, H. Shen, M. Wraback, D. Lubyshev, Y. Qiu, J. M. Fastenau, A. W. K. Liu, S. Elhamri, O. O. Cellek, and Y.-H. Zhang, "Significantly improved minority carrier lifetime observed in a long-wavelength infrared III-V type-II superlattice comprised of InAs/InAsSb", Appl. Phys. Lett. 99, 251110 (2011).
[12] D. Z.-Y. Ting, C. J. Hill, A. Soibel, S. A. Keo, J. M. Mumolo, J. Nguyen, and S. D. Gunapala, "A high-performance long wavelength superlattice complementary barrier infrared detector," Appl. Phys. Lett. 95, 023508 (2009).
[13] H. Kroemer, "A proposed class of heterojunction injection lasers," Proc. IEEE 51(12), 1782 (1963).
[14] Zh. I. Alferov, R. F. Kazarinov, Inventor's Certificate No. 181737 (in Russian), Application No. 950 840 (1963).
[15] A. M. White, "Infrared detectors," U. S. Patent No. 4,679,063 (7 July 1987).
[16] P. C. Klipstein, Y. Livneh, A. Glozman, S. Grossman, O. Klin, N. Snapi, and E. Weiss, "Modeling InAs/GaSb and InAs/InAsSb Superlattice Infrared Detectors", J. Electron. Mater. 43, 2984 (2014).
[17] S. Maimon and G. W. Wicks, "InAsSb/GaAlSb/InAsSb nBn IR detector for the 3-5μm", p.70, Program and Abstracts, 11th International Conference on Narrow Gap Semiconductors, June 16-20, 2003, Buffalo, New York.
[18] S. Maimon, "Reduced dark current photodetector", United States Patent Application No: US 2007/0215900 A1, (20 September 2007).
[19] J. R. Pedrazzani, S. Maimon and G. W. Wicks, "Use of nBn structures to suppress surface leakage currents in unpassivated InAs infrared photodetectors", Electronics Lett. 44(25) 1487-1488 (2008).
[20] David Z Ting, Alexander Soibel, Arezou Khoshakhagh, Linda Höglund, Sam A Keo, Sir B. Rafol, Cory J Hill, Anita M Fisher, Edward M Luong, Jean Nguyen, John K Liu, Jason M Mumolo, Brian J Pepper, Sarath D Gunapala, "Antimonide type-II superlattice barrier infrared detectors", SPIE Defense+ Security, 101770N-101770N-10, (2017).
[21] K. K. Choi, J. Sun, E. A. DeCuir, K. A. Olver, P. Wijewarnasuriya, "Electromagnetic Modeling and Resonant detectors and Arrays", Inf. Phys. & Tech. 70 (2015) 153–161. http://dx.doi.org/10.1016/j.infrared.2014.09.009.
[22] K. K. Choi, S. C. Allen, J. G. Sun, Y. Wei, K. A. Olver, R. X. Fu, "Resonant structures for infrared detection", Appl. Opt., 56, B26-B36, (2017).
[23] K. K. Choi, S. C. Allen, J. G. Sun, E. A. DeCuir, "Resonant detectors and focal plane arrays for infrared detection", Infra. Phys. & Tech., (2016), http://dx.doi.org/10.1016/j.infrared.2016.12.005.
[24] Kenneth I. Schultz, Michael W. Kelly, Justin J. Baker, Megan H. Blackwell, Matthew G. Brown, Curtis B. Colonero, Christopher L. David, Brian M. Tyrrell, and James R. Wey, "Digital-Pixel Focal Plane Array Technology", LINCOLN LABORATORY JOURNAL, Vol. 20 (2), 36-51 (2014).
[25] M. W. Kelly, R. Berger, *et al*., "Design and Testing of an All-Digital Readout Integrated Circuit for Infrared Focal Plane Arrays," Proc. SPIE, 5902, (2005).